Cancer Research

SMYD3-Mediated H2A.Z.1 Methylation Promotes Cell Cycle and Cancer Proliferation

Cheng-Hui Tsai[1], Yun-Ju Chen[1], Chia-Jung Yu[2,3], Shiou-Ru Tzeng[4], I-Chen Wu[4], Wen-Hung Kuo[5], Ming-Chieh Lin[6], Nei-Li Chan[4], Kou-Juey Wu[7], and Shu-Chun Teng[1]

Abstract

SMYD3 methyltransferase is nearly undetectable in normal human tissues but highly expressed in several cancers, including breast cancer, although its contributions to pathogenesis in this setting are unclear. Here we report that histone H2A.Z.1 is a substrate of SMYD3 that supports malignancy. SMYD3-mediated dimethylation of H2A.Z.1 at lysine 101 (H2A.Z.1K101me2) increased stability by preventing binding to the removal chaperone ANP32E and facilitating its interaction with histone H3. Moreover, a microarray analysis identified cyclin A1 as a target coregulated by SMYD3 and H2A.Z.1K101me2. The colocalization of SMYD3 and H2A.Z.1K101me2 at the promoter of cyclin A1 activated its expression and G_1–S progression. Enforced expression of cyclin A1 in cells containing mutant H2A.Z.1 rescued tumor formation in a mouse model. Our findings suggest that SMYD3-mediated H2A.Z.1K101 dimethylation activates cyclin A1 expression and contributes to driving the proliferation of breast cancer cells. *Cancer Res; 76(20); 6043–53.* ©*2016 AACR.*

Introduction

Chromatin changes, such as gene promoter methylation and post-translational modifications (PTM) of histones, have been linked to cancers (1–3). As more than 50 human histone methyltransferases (HMT) have been identified (4), understanding the functions of histone methylation has become a crucial issue. Studies have found that overexpression of HMTs that are responsible for the transcription-repressive marks, such as H3K9 and H3K27 methylation, leads to the aberrant silencing of tumor suppressor genes. For example, EZH2, a H3K27 HMT, and G9a, a H3K9 HMT, are upregulated in various cancers (5–7). In addition to repression-associated histone marks, MLL, a HMT for H3K4, modulates expression of various homeotic (Hox) genes and plays a key role in leukemic progression (8). Dysregulation of HMTs such as copy number amplification or aberrant gene expression leads to imbalance in histone methylation pathways and thus the initiation/progression of cancer (9).

SMYD3 is a HMT that is overexpressed in breast, colorectal, prostate, and hepatocellular tumors (10–13). Overexpression of SMYD3 enhances cell growth and cancer invasion, while reduced SMYD3 expression results in growth suppression (11, 14). SMYD3 can methylate H3K4, H4K5, and H4K20 to promote oncogenes or repress tumor suppressor genes (11, 15–17). For example, SMYD3 promotes telomerase expression, which correlates with an increase in H3K4 methylation at the telomerase promoter (18). SMYD3 also methylates a nonhistone protein, MAP3K2, to facilitate Ras/Raf/MEK/ERK signaling (19). However, how SMYD3 promotes cancer cell proliferation is not clear.

H2A.Z is an oncogenic histone variant that is overexpressed in breast, colorectal, liver, and bladder cancers (20–23). Two isoforms of H2A.Z, H2A.Z.1 and H2A.Z.2, have been identified as products of two nonallelic genes (24, 25), and each can execute isoform-specific function. H2A.Z.1 is pivotal for hepatocarcinogenesis by selectively modulating cell cycle and EMT-regulatory proteins (22), whereas H2A.Z.2 is a mediator of cell proliferation and drug sensitivity in malignant melanoma (26). Moreover, the oncogenic function of H2A.Z may be mediated through PTMs on H2A.Z and/or different combinations of H2A.Z isoform with other epigenetic regulations (21, 27–32).

Here we report the identification of histone H2A.Z.1 as a new substrate of SMYD3. We found that SMYD3 methylated H2A.Z.1 at lysine 101 (H2A.Z.1K101), which is in the globular domain of H2A.Z.1. This modification increased H2A.Z.1 protein stability by interfering with its removal by ANP32E and strengthening its binding to histone H3. The microarray analysis indicated that cyclin A1 was an important target of SMYD3 and H2A.Z.1K101me2. We further demonstrated how H2A.Z.1K101me2 accelerates G_1–S transition and leads to breast cancer proliferation.

[1]Department of Microbiology, College of Medicine, National Taiwan University, Taipei, Taiwan. [2]Department of Cell and Molecular Biology, Chang Gung University, Tao-Yuan, Taiwan. [3]Department of Thoracic Medicine, Chang Gung Memorial Hospital, Linkou, Tao-Yuan, Taiwan. [4]Institute of Biochemistry and Molecular Biology, College of Medicine, National Taiwan University, Taipei, Taiwan. [5]Department of Surgery, National Taiwan University Hospital, College of Medicine, National Taiwan University, Taipei, Taiwan. [6]Department of Pathology, National Taiwan University Hospital, College of Medicine, National Taiwan University, Taipei, Taiwan. [7]Research Center for Tumor Medical Science, Graduate Institute of Biomedical Sciences, China Medical University, Taichung, Taiwan.

Note: Supplementary data for this article are available at Cancer Research Online (http://cancerres.aacrjournals.org/).

C.-H. Tsai and Y.-J. Chen contributed equally to this article.

Corresponding Author: Shu-Chun Teng, Department of Microbiology, College of Medicine, National Taiwan University, No. 1, Sec. 1, Jen-Ai Road, Taipei 100, Taiwan. Phone: 8862-2312-3456, ext. 88289; Fax: 8862-2391-5293; E-mail: shuchunteng@ntu.edu.tw

doi: 10.1158/0008-5472.CAN-16-0500

Materials and Methods

Cell lines, plasmids, and transfection.

The breast cancer cell lines MCF7 and T47D were purchased from ATCC in 2012 and maintained in their respective media according to ATCC protocol. Cell line authentication was done by Food and Industry Research & Development Institute (Taiwan) using short random repeat DNA sequencing in 2016. Plasmid construction, virus preparation, and generation of transduced cell lines are described in the Supplementary Materials and Methods. The specific oligo sequences of shRNA are listed in Supplementary Table S2.

***In vitro* HMT assay**

The *in vitro* HMTase assay was performed as described with some modifications (11). Briefly, GST-tagged human SMYD3 and mutant SMYD3^{Y239F} proteins were purified from *E. coli*, and an *in vitro* HMT assay was performed with 10 μg of calf thymus histones (Sigma), recombinant histones, or purified nucleosomes isolated from shSMYD3 MCF7 cells (33) as substrates. To determine the methylated site of human H2A.Z.1, recombinant His-tagged H2A.Z.1 and GST-tagged SMYD3 were coincubated with cold *S*-adenosyl-L-methionine (SAM, Sigma). The LC/MS-MS was employed to identify the methylated sites of histones.

Isothermal titration calorimetry experiments

Calorimetric titrations of GST-ANP32E with H2A.ZK101 and H2A.ZK101me2 peptides were performed on an iTC200 microcalorimeter (GE) at 20°C and 30°C for determination of binding enthalpy and affinity. Protein samples were extensively dialyzed against the isothermal titration calorimetry (ITC) buffer containing 25 mmol/L KPi (pH 8.0), 250 mmol/L KCl, and 1 mmol/L Tris (2-carboxyethyl)phosphine (TCEP). The 200-μL sample cell was filled with a 100 μmol/L solution of protein and the 40-μL injection syringe, with 1.6 mmol/L of the titrating peptides. The titration data were analyzed using the program Origin 7.0 and nonconstrained fitting was performed for the interaction of GST-ANP32E with peptides. For more details, see the Supplementary Materials and Methods.

Histone eviction assay

Eviction assay was performed using immunoprecipitated Flag-H2A.Z–containing nucleosomes that were incubated with increasing amount of recombinant GST-ANP32E. Bound and unbound materials were blotted with either anti-H3 or anti-Flag antibodies. For more details, see the Supplementary Materials and Methods.

Mouse xenograft model

For each condition, 1×10^6 MCF7 cells were harvested in 100-μL PBS and injected subcutaneously on both sides of the back in 4-week-old female nude mice ($n = 6$). Tumor size was measured weekly and calculated with the formula length × width^2/2. Tumor incidence was defined when the tumor mass reached 100 mm^3, and growth was monitored until it reached 500 mm^3. After 10 weeks, the mice were sacrificed and the xenografts were excised and weighed.

Study approval

All the experiments involving mice were performed in accordance with the protocols approved by the Institutional Animal Care and Use Committee (IACUC) of National Taiwan University College of Medicine and College of Public Health (IACUC no. 20120046). Detailed methods are provided in Supplementary Materials and Methods.

Results

SMYD3 methylates H2A.Z.1 *in vitro* and *in vivo*

SMYD3 has been reported to methylate several histones including H3K4, H4K5, and H4K20 (11, 15, 16). To identify novel substrates of SMYD3, we used recombinant SMYD3 and catalytic dead mutant SMYD3^{Y239F} proteins (34) to perform an *in vitro* HMT assay on calf thymus histone extracts. The autoradiography analysis demonstrated that multiple histone proteins were detected as the potential substrates of SMYD3 (Fig. 1A). This result was consistent with our LC/MS-MS data, in which several well-known substrates of SMYD3 were identified (Supplementary Table S1). Interestingly, bovine H2A.Z (the human H2A.Z.1 homolog) methylation was identified in the mass data. To examine the specificity, we first confirmed that SMYD3^{WT}, but not the SMYD3^{Y239F}, also methylated recombinant human H2A.Z.1 (Fig. 1B). In addition, compared with H2A.Z.1, H4 was a better substrate, but H3 was not so preferable for SMYD3 (Fig. 1B). LC/MS-MS assay identified that lysine 101 of human H2A.Z.1 was monomethylated (H2A.Z.1K101me) and dimethylated (H2A.Z.1K101me2) by SMYD3 (Supplementary Fig. S1). However, the proportion of methylated protein *in vivo* was difficult to estimate. An *in vitro* HMT assay confirmed that H2A.Z.1^{K101Q} and H2A.Z.1^{K101R} mutants, in which the lysine residue was replaced with glutamine and arginine, respectively, were unable to be methylated by SMYD3 (Fig. 1C). Next, a lentiviral shRNA infection system was employed to knockdown SMYD3 (shSMYD3) in cells. When nucleosomes isolated from shSMYD3 MCF7 cells were used as substrates, a signal between H3 and H4 was detected (Supplementary Fig. S2A). We further generated an H2A.Z methylation–specific antibody. This antibody recognized only H2A.ZK101me2 peptide but not H2A.Z peptide without methylation (Supplementary Fig. S2B). The H2A.ZK101me2 antibody detected three signals from total lysates of MCF7 cells. Only the 14-kDa signal, the predicted molecular weight of H2A.Z, disappeared upon preincubation of H2A.ZK101me2 antibody with H2A.ZK101me2 peptide (Supplementary Fig. S2C). Furthermore, the antibody could detect exogenously expressed H2A.Z^{WT} but not H2A.Z^{K101Q} and H2A.Z^{K101R} (Supplementary Fig. S2D), suggesting that the detected signal was the H2A.ZK101me2 protein. When nucleosomes isolated from shSMYD3 MCF7 cells were used as substrates, SMYD3 increased the methylation level of K101 (Fig. 1D), suggesting that SMYD3 could methylate H2A.Z in the context of nucleosome. Interestingly, SMYD3 also increased H3K4 and H4K20 methylation but not that of H4K5 (Supplementary Fig. S2E). In addition, when examining H2A.ZK101me2 protein levels in shSMYD3 T47D and MCF7 breast cancer cell lines, the H2A.ZK101me2 level was reduced in SMYD3 knockdown cells, while the protein level of H2A.Z remained similar (Fig. 1E and Supplementary Fig. S2F). Consistently, overexpression of SMYD3^{WT} elevated the level of H2A.ZK101me2 by 60% in 293T cells (Fig. 1F). Together, these findings indicate that H2A.Z is very likely an *in vivo* substrate of SMYD3.

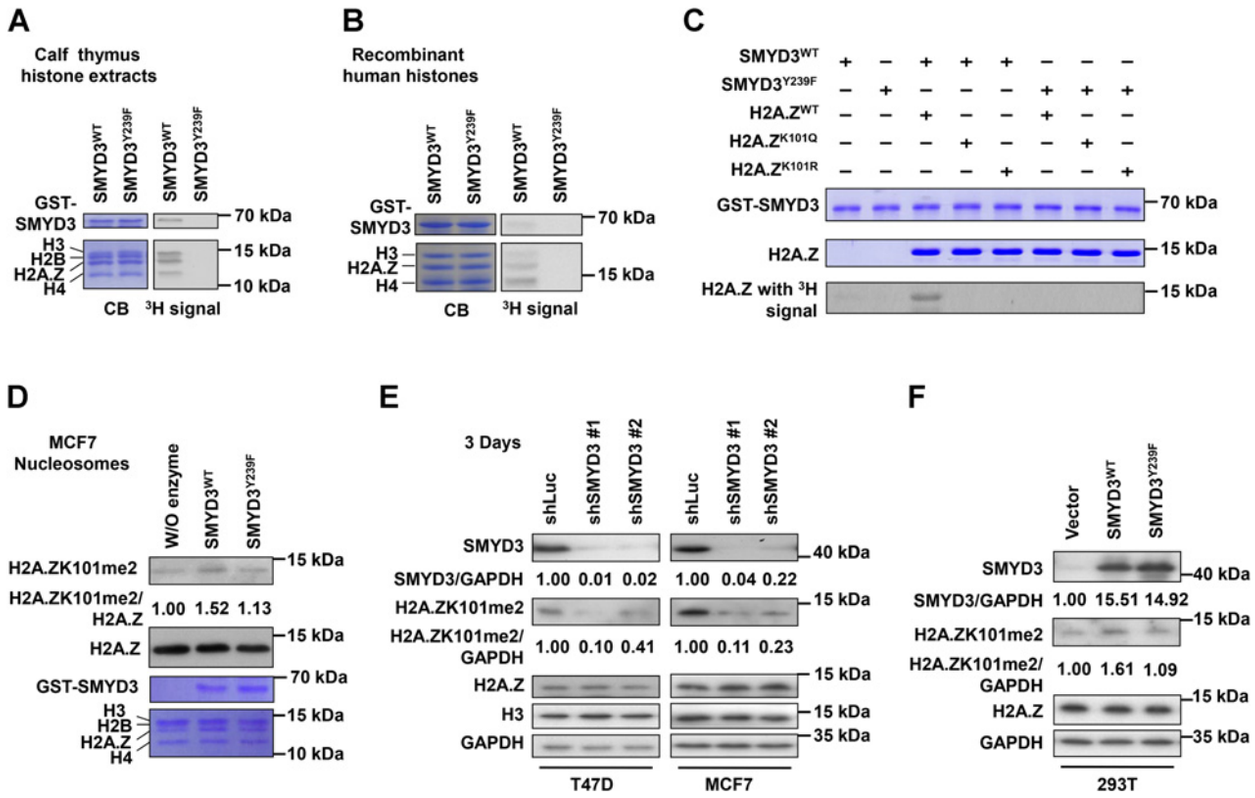

Figure 1.

SMYD3 methylates H2A.Z.1K101 *in vitro* and *in vivo*. **A–D,** *in vitro* HMT assays of GST-tagged human SMYD3^{WT} and SMYD3^{Y239F}. Calf thymus histone extracts (**A**) and recombinant His-tagged human H2A.Z.1, H3, and H4 (**B**) were used as substrates. **C,** recombinant H2A.Z^{WT}, H2A.Z^{K101Q}, and H2A.Z^{K101R} were used as substrates. Coomassie blue staining indicated equal loading and autoradiography is shown. **D,** nucleosomes isolated from 3-day SMYD3 knockdown MCF7 cells were used as substrates. Western blotting were conducted using indicated antibodies. Coomassie blue staining indicated equal loading of GST-tagged human SMYD3^{WT}, SMYD3^{Y239F}, and isolated nucleosomes. **E,** T47D and MCF7 cells were infected with lentiviruses carrying shLuc control vector or shSMYD3 for 3 days. **F,** 293T cells overexpressing SMYD3^{WT} or SMYD3^{Y239F} proteins. In **E** and **F,** Western blotting was conducted using indicated antibodies. The ratio of individual protein relative to the loading control GAPDH is indicated below. All data are representative of $n \geq 3$ for each experiment.

SMYD3-mediated K101 methylation maintains the association of H2A.Z protein with chromatin

Previous studies demonstrated that deletion of the acidic patch, which contains K101, resulted in more dynamic association with chromatin and lower H2A.Z occupancy at target genes (35–37). To examine whether dimethylation of H2A.Z influences its association with chromatin, nuclei isolated from shLuc control or shSMYD3 cells were subjected to salt titration (Fig. 2A). Western blotting demonstrated that while H2A.Z in shLuc cells was stably associated with chromatin in up to 0.6 mol/L NaCl and partially depleted at 0.8 mol/L NaCl (dissociation of H2A.Z/H2B dimer usually occurs between 0.6 and 0.8 mol/L NaCl; refs. 38, 39), a fraction of H2A.Z in shSMYD3 cells dissociated at lower salt concentrations (0.4–0.6 mol/L NaCl; Fig. 2B). Consistently, a similar feature was observed in H2A.Z-mutant cells that H2A.Z^{K101Q} and H2A.Z^{K101R} were less tightly associated with chromatin than H2A.Z^{WT} (Fig. 2C and D). Finally, whether dimethylation of H2A.Z exerted any effect on chromatin structure remained unclear. SMYD3 knockdown cells or H2A.Z^{WT}, H2A.Z^{K101Q}, and H2A.Z^{K101R}-expressing MCF7 cells were subjected to micrococcal nuclease (MNase) digestion. No significant difference in the cleavage pattern was observed, implying that the absence of SMYD3 or the methylation status of H2A.Z does not affect global chromatin compaction (Fig. 2E and F).

Dimethylation of H2A.Z hinders ANP32E-mediated H2A.Z removal and enhances its affinity with histone H3

The chromatin remodeler such as SRCAP (Snf2-related CREBBP activator protein) and TIP60–p400 complex mediates site-specific incorporation of H2A.Z in mammalian cells (27, 40, 41). Moreover, the H2A.Z-deposition chaperone, YL1 (30), and the H2A.Z-eviction chaperone, ANP32E (29, 42), are important for H2A.Z nucleosome association. In view of this, we tested the ability of H2A.Z^{K101Q} and H2A.Z^{K101R} to interact with these complexes and chaperones. A coimmunoprecipitation assay was performed with an anti-Flag antibody against Flag-tagged H2A.Z^{WT}, H2A.Z^{K101Q}, and H2A.Z^{K101R} proteins. Similar amounts of the two SRCAP subunits (SRCAP and RUVBL1), two TIP60-p400 subunits (TIP60 and p400), and YL1 were coprecipitated with H2A.Z^{WT} and H2A.Z^{K101} mutants (Fig. 3A and Supplementary Fig. S3A), suggesting that the abilities of SRCAP-, TIP60-p400-, and YL1-mediated deposition of H2A.Z proteins were not altered in mutant cells. Conversely, H2A.Z^{K101} mutants displayed a higher affinity to ANP32E

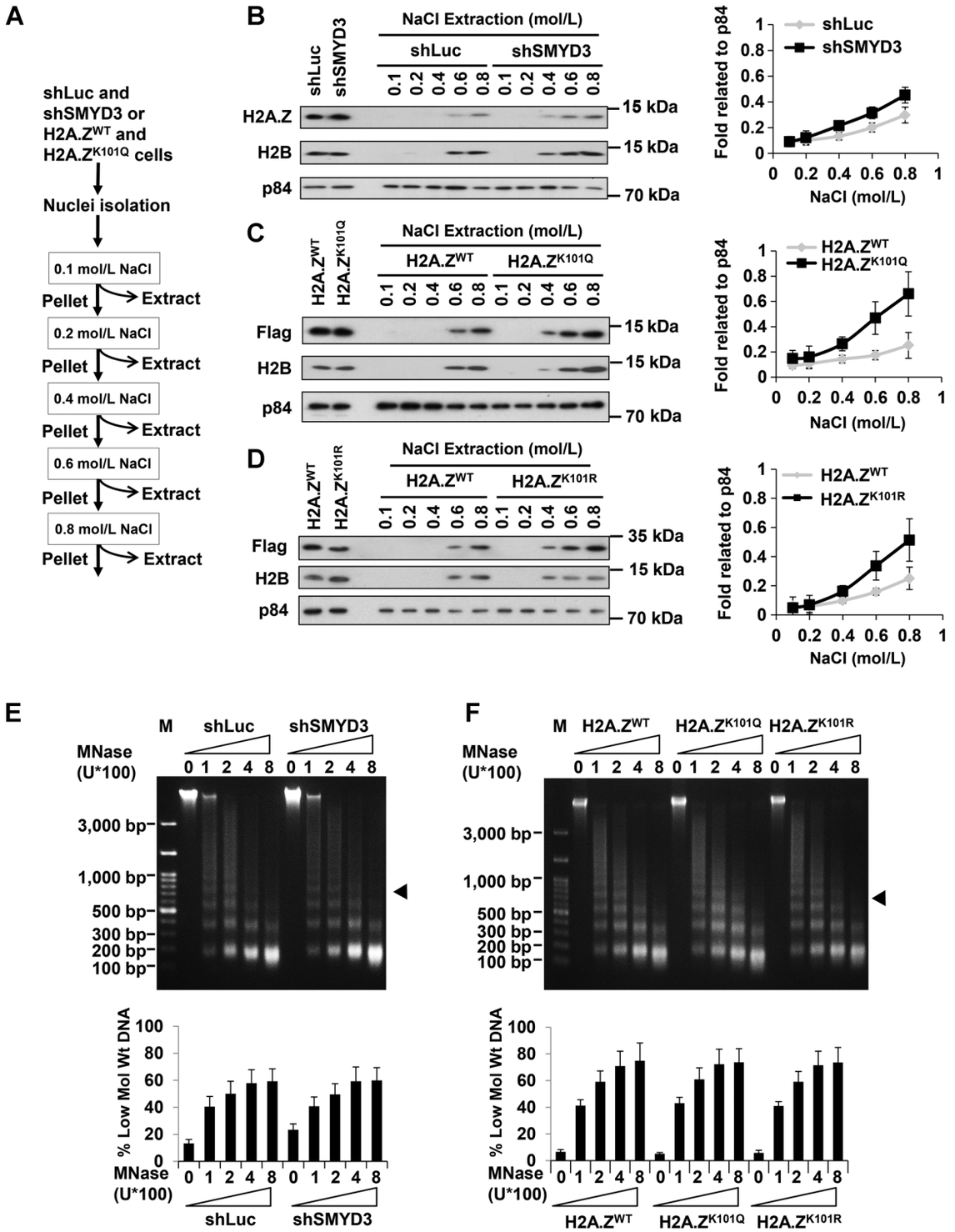

Figure 2.

SMYD3-mediated K101 methylation maintains H2A.Z association with chromatin. **A,** schematic view of salt wash assay. **B–D,** nuclei isolated from shLuc control and SMYD3 knockdown (**B**) or H2A.Z^{WT}-, H2A.Z^{K101Q}- (**C**), and H2A.Z^{K101R}(**D**)-expressing MCF7 cells were subjected to increasing salt concentrations. Western blotting was performed using indicated antibodies. Right, the ratio of endogenous H2A.Z or H2A.Z-Flag protein relative to p84 is illustrated. **E** and **F,** nuclei isolated from shLuc or shSMYD3 (**E**) or H2A.Z^{WT}-, H2A.Z^{K101Q}-, and H2A.Z^{K101R}-expressing (**F**) MCF7 cells were subjected to increasing MNase concentrations. Digested chromatin DNA was resolved by gel electrophoresis. The proportion of low molecular weight DNA (< tetranucleosome) was calculated as a percentage of the total sample in each lane. All values in the histograms are means ± SD of triplicates and data are representative of $n \geq 3$ for each experiment.

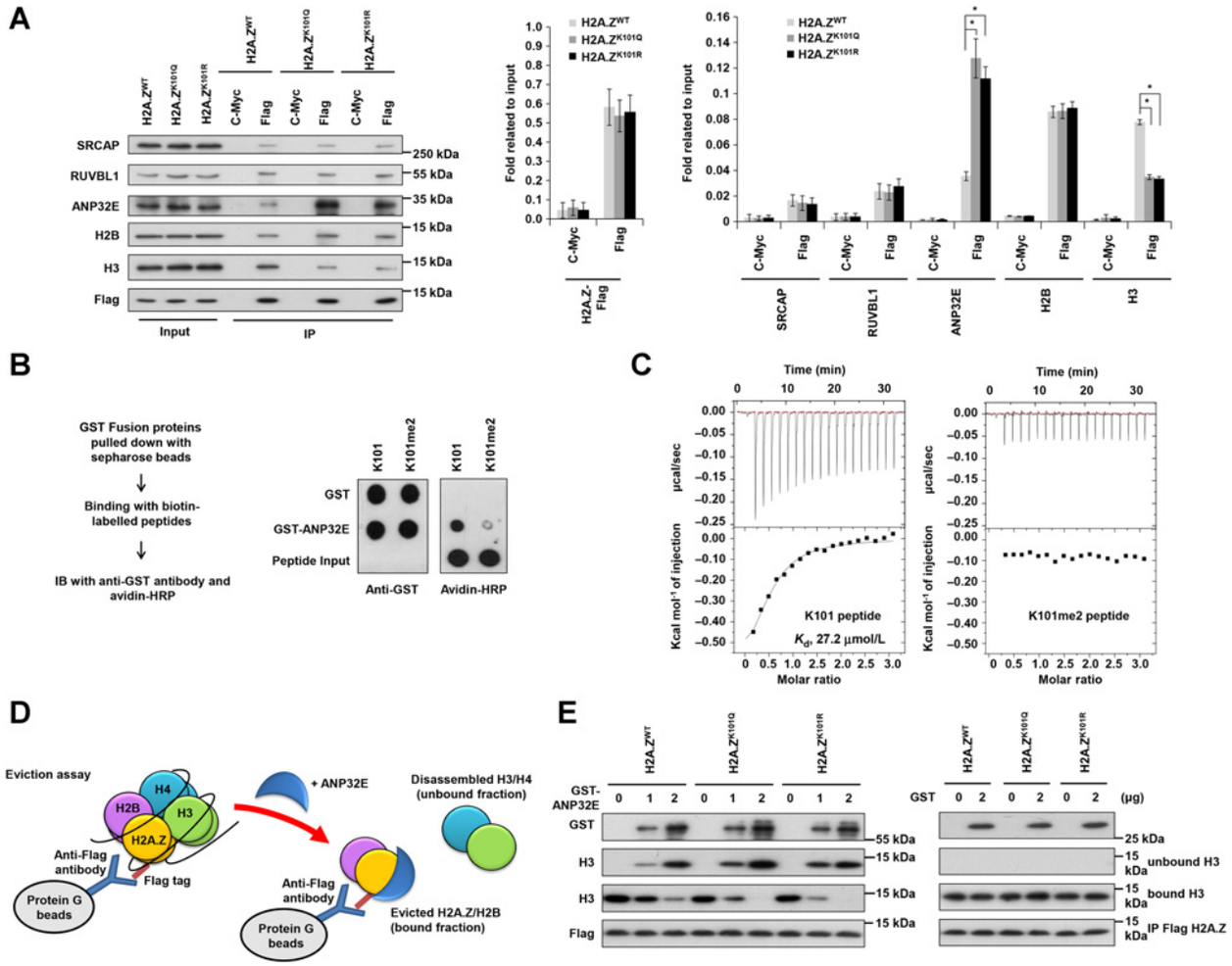

Figure 3.

Dimethylation of H2A.Z modulates its binding to ANP32E and histone H3. **A,** coimmunoprecipitation from endogenous H2A.Z-knocked down H2A.Z^{WT}-, H2A.Z^{K101Q}-, and H2A.Z^{K101R}-expressing MCF7 cells with an anti-Flag antibody. The histograms show the ratio of individual protein signal to their input signal in Western blots. *, $P < 0.05$. **B,** a scheme of the GST-ANP32E pull-down assay (left). Right, the anti-GST dot blot shows equally pulled-down GST or GST-ANP32E. The avidin–HRP dot blot shows that GST-ANP32E co-pulled down more nonmethylated H2A.Z (K101) than dimethylated peptides (K101me2). Peptides (100 ng) were spotted as the input controls. **C,** calorimetric titration of K101 (left) or K101me2 peptides (right) into GST-ANP32E. Top, raw data of the heat released. Bottom, binding isotherm of the reaction. **D,** a scheme of eviction assay. The Flag pulled-down nucleosomes were immobilized on protein G beads and incubated with GST-ANP32E. ANP32E disassembles nucleosomes, which causes the release of histone H3 (unbound fraction). **E,** bound and unbound histones were analyzed by Western blotting. All values in the histograms are means ± SD of triplicates and data are representative of $n \geq 3$ for each experiment.

compared with H2A.Z^{WT} (Fig. 3A). An *in vitro* GST-ANP32E pull-down experiment using biotinylated H2A.Z peptides containing amino acids 93–108 revealed that ANP32E bound directly to H2A.Z, with a preference for K101 to K101me2 (Fig. 3B).

To evaluate the interactions between ANP32E and peptides in quantitative terms, we measured the dissociation constants by ITC. ITC assay showed that H2A.ZK101 peptides bound to ANP32E with a K_d of 27.2 µmol/L (Fig. 3C, left), whereas H2A.ZK101me2 peptides displayed no detectable binding for GST-ANP32E (Fig. 3C, right and Table 1). These findings further confirmed that dimethylated H2A.Z inhibits the interaction between H2A.Z and ANP32E. Previous studies have shown that ANP32E was able to specifically remove H2A.Z from the nucleosome (29, 42). To test whether H2A.ZK101me2 could reduce histone displacement from chromatin, we performed a histone eviction assay (Fig. 3D). Flag-tagged H2A.Z^{WT} and H2A.Z^{K101}-mutant–containing nucleosomes were immunoprecipitated and then incubated with increasing amounts of recombinant GST-ANP32E or GST alone as a negative control. The bound histones and unbound material were subjected to Western blotting with anti-H3 or anti-Flag antibodies. Disassembled nucleosomes resulted in release of histones H3 and H4 while H2A.Z-H2B dimers remained bound to the beads. As expected, less histone H3 was detected in the evicted fraction from H2A.Z^{WT} than that from the H2A.Z^{K101}-mutant–containing nucleosomes (Fig. 3E), suggesting that the H2A.Z dimethylation decreases histone displacement/eviction on chromatin.

Table 1. Thermodynamic parameters in the interaction between ANP32E and H2A.Z peptides as measured by ITC

Peptide sequence	T, °C	K_a, 10^3/M	K_d, μmol/L	ΔG, kcal/mol	ΔH, kcal/mol	−TΔS, kcal/mol	N	Ligand, mmol/L	Protein, mmol/L
DEELDSLIKATIAGGGVGGK	20	36.7	27.2	−6.11	−0.752	−5.36	0.7	1.6	0.1
DEELDSLIKATIAGGGVGGK	30	35.4	28.2	−6.30	−0.452	−5.88	0.84	1.6	0.1
DEELDSLIK(me2)ATIAGGGVGGK	20	NBD	NBD	NBD	NBD	NBD	NBD	1.6	0.1
DEELDSLIK(me2)ATIAGGGVGGK	30	NBD	NBD	NBD	NBD	NBD	NBD	1.6	0.1

Abbreviations: K_a, association constant; K_d, dissociation constant; N, the stoichiometry of the interaction; NBD, no binding detectable.

We further verified the interaction between H2A.Z and other histones, including histone H2B, which forms a dimer with H2A.Z, and histone H3, which directly interacts with H2A.Z via hydrogen bonds to stabilize nucleosomes (43). Interestingly, while the affinity between H2A.Z^{K101} mutants and H2B remained the same (Fig. 3A), H2A.Z^{K101} mutants exhibited decreased association with H3 both *in vitro* and *in vivo* (Fig. 3A and Supplementary Fig. S3B). Similarly, using K101- or K101me2-biotinylated peptides to pull down endogenous interacting proteins, we confirmed that the interaction between ANP32E and the K101 peptide was greatly increased compared with that between ANP32E and the K101me2 peptide, whereas histone H3 exhibited stronger affinity with K101me2 than with K101 (Supplementary Fig. S3C). In SMYD3 knockdown cells, the interaction between ANP32E and H2A.Z was increased. Conversely, the interaction between H3 and H2A.Z was decreased (Supplementary Fig. S3D). These data imply that the dimethylation of H2A.ZK101 may serve as a signal to prevent the binding of H2A.Z to its chaperone that removes H2A.Z from chromatin, thus stabilizing the interaction between H2A.Z and H3.

Dimethylation of H2A.Z Lys101 is critical for promoting S-phase entry, cell proliferation, and tumorigenesis

SMYD3 (10–13) and H2A.Z (19–22) are overexpressed in several tumors. Consistently, we observed a positive correlation of expression between SMYD3 and H2A.ZK101me2 in a series of cancer cell lines and human breast tissue samples (Supplementary Fig. S4A and S4B). To further investigate this correlation, we first knocked down endogenous H2A.Z.1 and the growth of H2A.Z.1 knockdown MCF7 cells was compromised. H2A.Z.1^{WT} expression was able to restore delayed cell growth, whereas H2A.Z.1^{K101Q} or H2A.Z.1^{K101R} failed to do that (Fig. 4A and Supplementary Fig. S4C). Consistent with MCF7 cells, H2A.Z^{WT} T47D cells grew much faster than cells expressing empty vectors or H2A.Z^{K101Q} (Fig. 4B). The effect of H2A.Z on cell proliferation was more prominent in T47D cells. Therefore, we further examined cell-cycle progression of T47D cells. H2A.Z^{WT} cells entered the S-phase rapidly at 8 hours and proceeded through the cell cycle, but H2A.Z^{K101Q} failed to accelerate cell-cycle progression (Fig. 4B). These results suggested that the methylation of H2A.Z at K101 is critical for S-phase entry and cell proliferation. To test whether K101 mutation affected H2A.Z-mediated tumorigenic activity, colony formation was analyzed in H2A.Z^{WT}, H2A.Z^{K101Q}, and H2A.Z^{K101R}-expressing MCF7 cells when endogenous H2A.Z expression was suppressed. Compared with H2A.Z^{WT} cells, H2A.Z^{K101Q} and H2A.Z^{K101R} cells could neither increase the number of colonies nor rescue the colony formation defect caused by H2A.Z knockdown (Fig. 4C). When H2A.Z^{K101Q} and H2A.Z^{K101R} cells were subcutaneously injected into nude mice, the tumor volumes were significantly smaller than those formed by H2A.Z^{WT} cells (Fig. 4D, right), even though H2A.Z^{WT}, H2A.Z^{K101Q}, and H2A.Z^{K101R} proteins were constitutively expressed at equal amounts in isolated tumors after 10 weeks (Fig. 4D, left). The soft agar assay revealed that knockdown of SMYD3 decreased the tumorigenic activity of H2A.Z^{WT} (Supplementary Fig. S4D). In addition, knockdown of SMYD3 also lowered the proliferation advantage of H2A.Z^{WT} cells (Fig. 4E). Furthermore, SMYD3 overexpression promoted the proliferation of MCF7 cells (Supplementary Fig. S4E). Compared with that of H2A.Z^{WT} cells, SMYD3 overexpression could not promote the proliferation of H2A.Z^{K101Q} cells in the endogenous H2A.Z knockdown MCF7 background (Fig. 4F, lane 2 vs. lane 4 and lane 6 vs. lane 8). Overexpression of both H2A.Z^{WT} and SMYD3 did not display cooperative effect on cell proliferation (Supplementary Fig. S4F, lane 4 vs. lane 2). These results suggest that hindered methylation on H2A.ZK101 disrupts the oncogenic potential of H2A.Z.

SMYD3 and H2A.ZK101me2 activate cyclin A1 expression

To identify the target genes of SMYD3-mediated H2A.ZK101me2, whole-genome microarray analysis of RNA isolated from two parallel experiments, including shLuc versus shSMYD3 cells (GEO accession number GSE58048) and H2A.Z^{WT} versus H2A.Z^{K101Q} in endogenous H2A.Z knockdown MCF7 cells (GEO accession number GSE58047), were conducted. We found that the expressions of 996 transcripts were altered upon SMYD3 knockdown (Supplementary Fig. S5A). The gene ontology (GO) analysis indicated that these 996 SMYD3-regulated transcripts were involved in cell cycle, organelle fission, and cell division (Supplementary Fig. S5B), which was consistent with previous reports (11, 44). In addition, 245 transcripts were altered by H2A.Z when K101 was mutated to Q (Supplementary Fig. S5A). In agreement with the multifunctional roles of H2A.Z (45), the GO analysis showed that the majority of H2A.ZK101-regulated genes were involved in nucleotide metabolism, regulation of blood vessel size, defense-related response, and vasodilation (Supplementary Fig. S5C). Most importantly, only 35 transcripts, which belong to 19 genes, were coregulated by SMYD3 and H2A.ZK101 (Supplementary Fig. S5A; Supplementary Table S2). Among these genes, 8 were downregulated and 11 were upregulated. To verify the accuracy of the microarray data, qRT-PCR was performed for these 19 genes. Most genes exhibited similar fold differences in mRNA expression as originally identified in the microarray analysis (Supplementary Fig. S5D and S5E).

As H2A.Z is known to promote cell growth (46), cyclin A1 (*CCNA1*), the only cell-cycle–controlled gene among the 19 genes coregulated by SMYD3 and H2A.ZK101me2, was further analyzed. Consistently, knockdown of SMYD3 (Fig. 5A) or H2A.Z (Fig. 5B) decreased the expression of cyclin A1. Moreover, expression of H2A.Z^{WT} or SMYD3^{WT} activated cyclin A1 protein level (Fig. 5C and Supplementary Fig. S4E, respectively). In contrast, the mRNA level of cyclin A2, another member in the cyclin A family, remained unchanged in H2A.Z knockdown cells (Supplementary Fig. S6A). Chromatin immunoprecipitation (ChIP) assays further indicated that the endogenous SMYD3 and

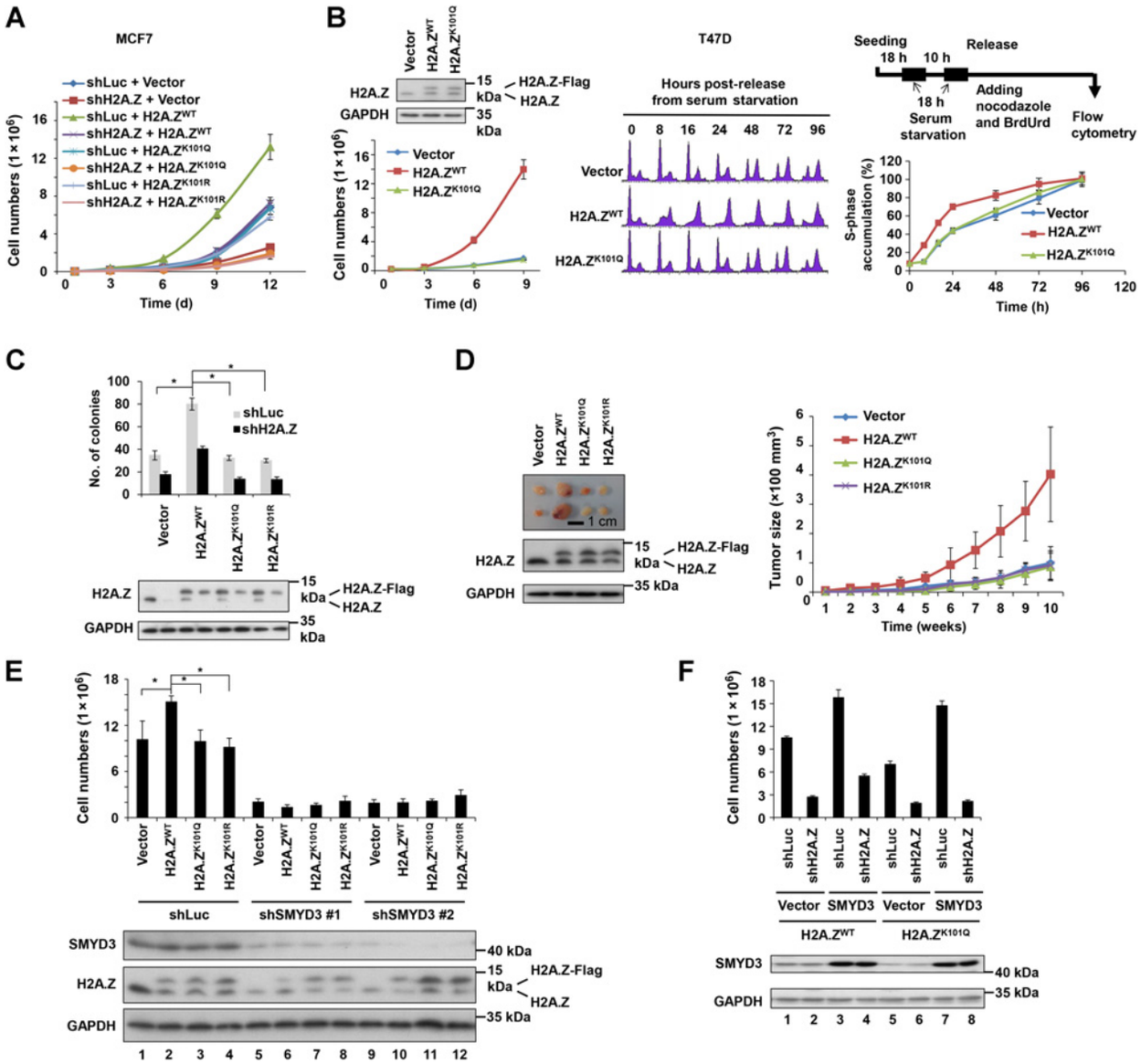

Figure 4.

H2A.ZK101 dimethylation is critical for promoting cell proliferation and tumorigenesis. **A,** H2A.Z-promoted MCF7 cell proliferation was abolished in H2A.Z^{K101Q}- and H2A.Z^{K101R}-expressing cells. **B,** left, growth of T47D cells overexpressing empty vector, H2A.Z^{WT}, or H2A.Z^{K101Q} proteins. Right, T47D cells were synchronized at G_1–S transition and released from arrest to observe cell-cycle progression. Percentage of cells accumulated at S-phase was quantified. **C,** numbers of colonies derived from cells with knockdown of endogenous H2A.Z and expression of empty vector, H2A.Z^{WT}, H2A.Z^{K101Q}, or H2A.Z^{K101R} were counted. **D,** indicated cells were injected into mice ($n = 6$). Tumor size was measured weekly. **E,** H2A.Z^{WT}-promoted MCF7 cell proliferation was abolished in SMYD3 knockdown cells as determined by counting number of cells on day 12. **F,** SMYD3-promoted MCF7 cell proliferation was abolished in H2A.Z^{K101Q}-expressing cells. Cell proliferation was measured on day 12. *, $P < 0.05$; **, $P < 0.01$. All values in the histograms are means ± SD of triplicates and data are representative of $n \geq 3$ for each experiment. BrdUrd, bromodeoxyuridine.

dimethylated H2A.Z associated specifically with the cyclin A1 promoter from -623 to -532 bp (region b) relative to the transcription start site (TSS; Fig. 5D). The net amounts of dimethylated H2A.Z and H2A.Z were enriched at region b compared with those at other regions (Fig. 5D). Moreover, a re-ChIP assay confirmed the colocalization of H2A.Z and H2A.ZK101me2 at the same region (Supplementary Fig. S6B), demonstrating the specificity of the anti-H2A.ZK101me2 antibody. Furthermore, knockdown of SMYD3 also decreased SMYD3, H2A.ZK101me2, and H2A.Z binding to region b of the cyclin A1 promoter, but not to the control region (Fig. 5E, region a). SMYD3 knockdown did not affect the localization of histones H2A, H2B, H3, and H4, except that H2B had an increased level at the control region for a currently unknown reason (Supplementary Fig. S6C and S6D). To test whether H2A.Z^{WT} associates more closely with chromatin than mutant H2A.Z, ChIP assays using anti-Flag antibody were

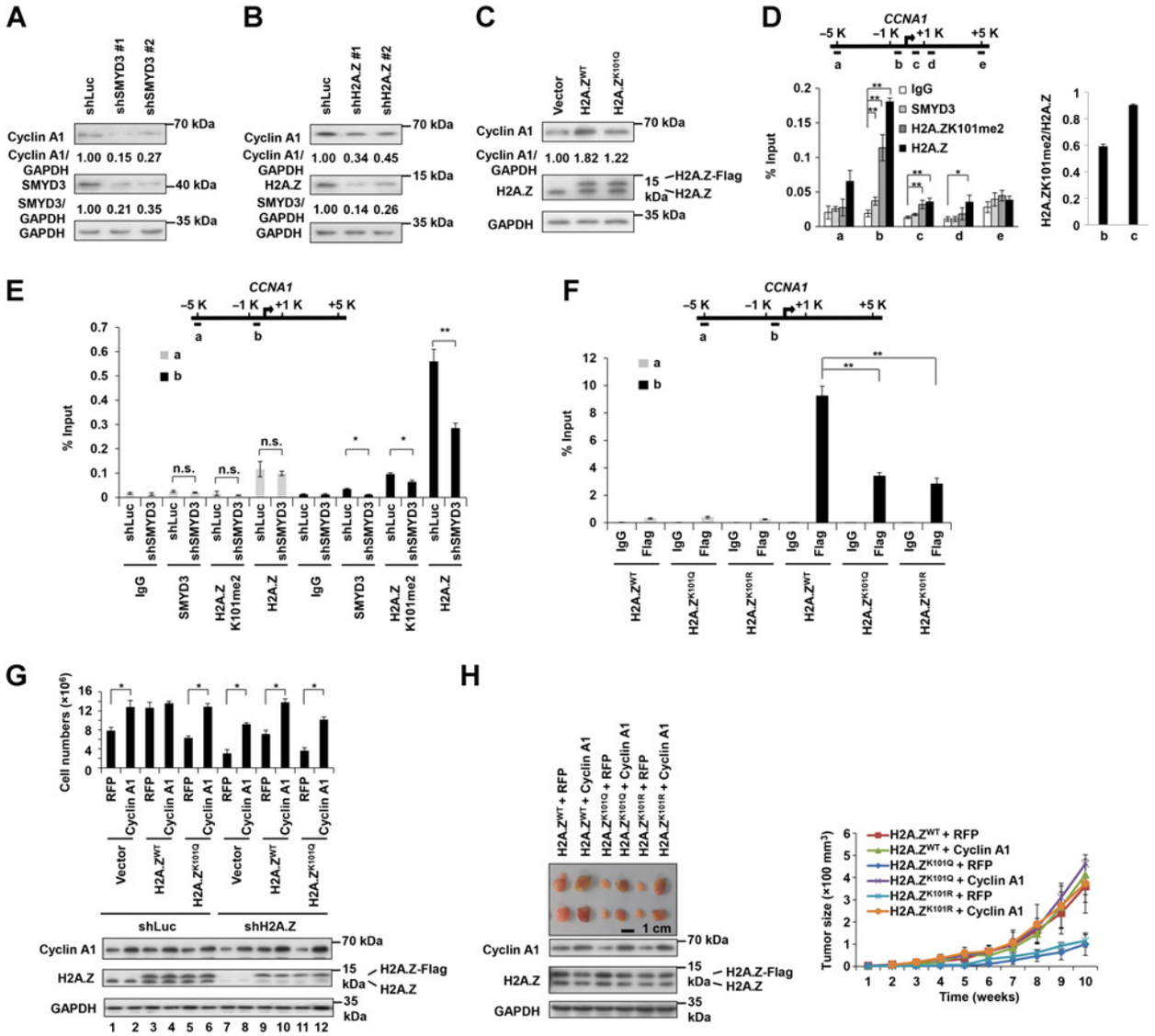

Figure 5.

Cyclin A1 is a downstream target of SMYD3 and H2A.ZK101me2. **A–C,** Western blotting of SMYD3-repressed (**A**), H2A.Z-repressed (**B**), or H2A.Z^{WT}- or H2A.Z-mutant–expressing (**C**) MCF7 cells. **D,** ChIP assay was performed in MCF7 cells using specific antibodies. Five examined positions at the cyclin A1 locus are indicated. Ratios of H2A.ZK101me2/H2A.Z ChIP signals in regions b and c of the cyclin A1 promoter are indicated. **E,** ChIP assay was performed with SMYD3-repressed MCF7 cells using specific antibodies. **F,** MCF7 cells expressing H2A.Z^{WT}, H2A.Z^{K101Q}, or H2A.Z^{K101R} were subjected to ChIP assay using anti-Flag antibody. In **D–F,** immunoprecipitated chromatin was quantified by qRT-PCR. **G,** MCF7 cells expressing H2A.Z^{WT} and H2A.Z^{K101Q} were subjected to Luc or H2A.Z knockdown and complemented with RFP control or cyclin A1. Cell proliferation assay was performed. **H,** indicated cells were injected into mice ($n = 6$) and tumor size was measured. n.s., not significant; *, $P < 0.05$; **, $P < 0.01$. All values in the histograms are means ± SD of triplicates and data are representative of $n \geq 3$ for each experiment.

performed. The presence of H2A.Z^{WT} was 2.72- and 3.28-fold higher than that of H2A.Z^{K101Q} and H2A.Z^{K101R}, respectively, at the target region of the cyclin A1 promoter (Fig. 5F, region b), but not at the control region (Fig. 5F, region a). In addition, the increased level of H2A.Z in H2A.Z^{WT} cells compared with that in H2A.Z-mutant cells further supported the role of H2A.Z dimethylation for its chromatin association (Supplementary Fig. S6E). In contrast, other core histone subunits were equally distributed at the cyclin A1 promoter (Supplementary Fig. S6F and S6G). Taken together, these data indicate that SMYD3 may activate cyclin A1 gene expression by binding directly to the cyclin A1 promoter and dimethylating the local H2A.Z at K101.

To investigate the role of cyclin A1 in SMYD3- and H2A.ZK101me2-promoted cell proliferation, cyclin A1 was knocked down in empty vector, H2A.Z^{WT}, or H2A.Z^{K101Q} cells, followed by a cell count. The results showed that knocking down cyclin A1 reduced H2A.Z^{WT}-promoted cell proliferation (Supplementary Fig. S6G). Conversely, exogenous expression of cyclin A1, but

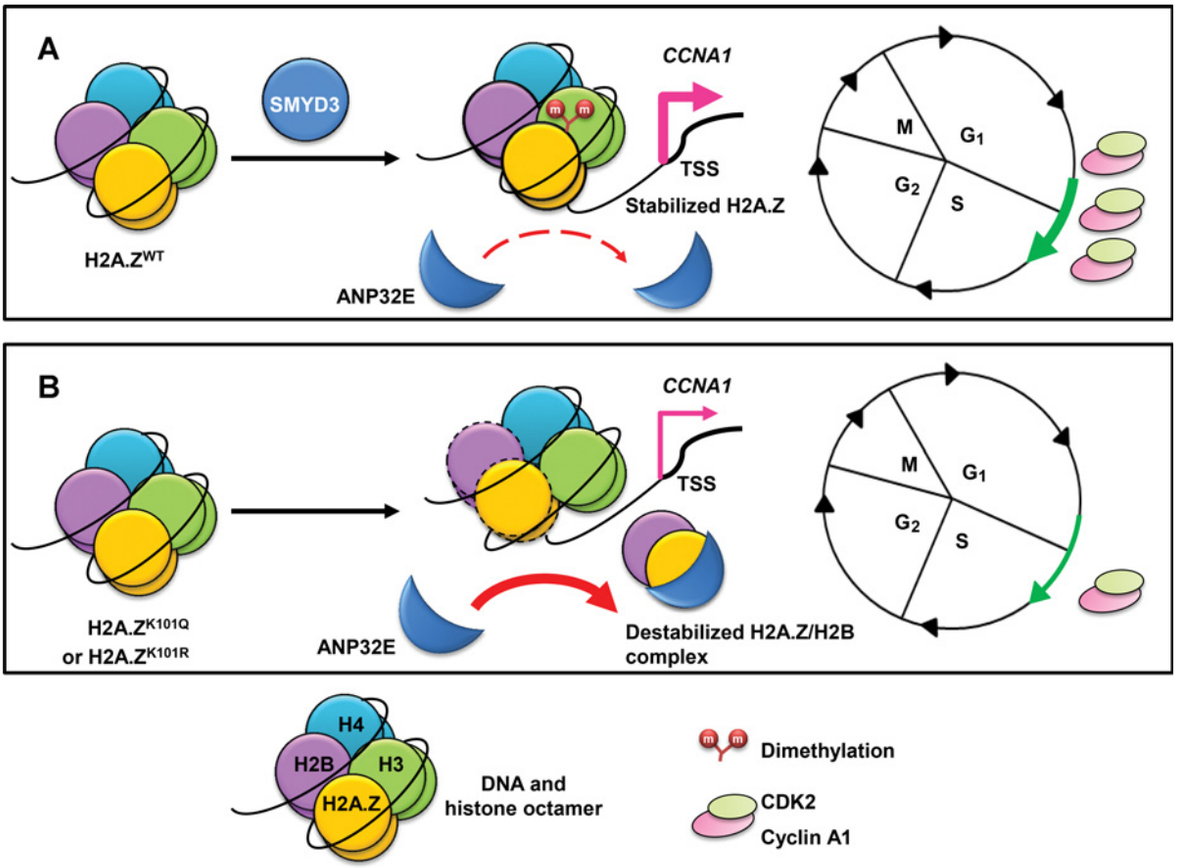

Figure 6.

SMYD3-catalyzed H2A.ZK101me2 couples chromatin dynamics to gene regulation at G_1–S transition. **A,** H2A.Z-containing nucleosomes can be methylated by SMYD3 at K101. H2A.ZK101me2 exhibits higher affinity with H3 and lower affinity with the removal chaperone ANP32E, thus stabilizing H2A.Z. Stabilized H2A.Z may mark the cyclin A1 promoter region and recruit the transcription machinery. Accumulated cyclin A1 protein therefore accelerates the G_1–S transition of cell cycle. **B,** H2A.Z^{K101} mutants cannot be methylated at K101. It is poorly associated with H3 and exerts higher affinity with ANP32E. Destabilized H2A.Z^{K101Q}/H2B or H2A.Z^{K101R}/H2B complex causes compromised cyclin A1 transcription and cell-cycle progression.

not the control with expression of red fluorescent protein (RFP), restored cell proliferation in H2A.Z^{K101Q} cells (Fig. 5G, lanes 5 and 6). In endogenous H2A.Z knockdown cells, the overexpression of cyclin A1 could rescue the compromised cell growth in vector control and H2A.Z^{K101Q} cells (Fig. 5G, lanes 8 and 12). Finally, the complementation of cyclin A1 in H2A.Z^{K101Q} cells significantly increased tumor growth in a mouse xenograft model (Fig. 5H). Taken together, these findings suggest that SMYD3-mediated dimethylation of H2A.Z at K101 can directly activate cyclin A1 expression and contribute to tumorigenesis.

Discussion

SMYD3 was originally identified as a methyltransferase that methylates histone H3K4 (11). Here, we identified a new substrate, histone H2A.Z.1, dimethylated at K101 by SMYD3 both *in vitro* and *in vivo*, but not by SMYD5 (Supplementary Fig. S6H). Although K101 is conserved in H2A and H2A.Z but not in H2A.X, H2A.Bbd and mH2A1.2, sequence diversity flanking K101 may alter the substrate specificity of SMYD3 (Supplementary Fig. S6I). In agreement with this, replacement of H2A amino acids 97-100 to H2A.Z decreased the ANP32E-H2A.Z association (28, 29). In addition, H2A.Z.1 can be methylated when it is in the free form (Fig. 1A–1C) or in the context of nucleosome (Fig. 1D). More importantly, H2A.Z.1 expression–stimulated cancer proliferation was prevented in H2A.$Z.1^{K101}$ mutant–expressing cells, suggesting that K101 dimethylation provides a major regulation for H2A.Z.1-driven cell proliferation (Fig. 6).

Our results showed that gene expression of several cell-cycle regulators, including *CCNA1*, *CCNA2*, *CCNB1*, and *CCNE2* were decreased in SMYD3 knockdown MCF7 cells. Another study observed that mRNA levels of *CcnA2*, *CcnD1*, and *CcnE1* were decreased in *Smyd3-KO* mice. Therefore, cyclin A2 seems to be regulated by SMYD3 in both human and mouse probably though H3K4me3 (13) but not H2A.ZK101me2 (Supplementary Fig. S6A). SMYD3 has been proposed to bind to specific DNA sequence, estrogen response elements, and conserved noncoding DNA sequence (11, 17, 47). Consistently, 11 of 19 qRT-PCR–confirmed genes contain these sequences/elements in their promoter regions (Supplementary Table S2). Even though SMYD3 usually performs as a transcriptional activator, 452 transcripts were upregulated upon SMYD3 knockdown. It is possible that

SMYD3 may drive some other factors to suppress these genes indirectly, or SMYD3-mediated H4K20 trimethylation may invoke gene repression (16). Further analysis by ChIP-seq may clarify whether SMYD3 and H2A.ZK101me2 transcriptionally regulate these genes through localizing to their promoters.

Our data demonstrated that H2A.Z^{K101} mutants and the non-methylated H2A.Z peptide exhibited stronger association with ANP32E than H2A.Z^{WT} and the H2A.ZK101me2 peptide, respectively (Fig. 3). Interestingly, the net amounts of promoter-associated H2A.Z increased by 20% in ANP32E-knockout cells (29), which is consistent with our finding that the increased association between H2A.Z^{K101} mutants and ANP32E decreases the presence of H2A.Z^{K101Q} and H2A.Z^{K101R} at the cyclin A1 promoter (Fig. 5F). Furthermore, stronger affinity between H2A.Z^{WT} and histone H3 than that between H2A.Z^{K101} mutants and histone H3 supports the hypothesis that K101 dimethylation increases the stability of H2A.Z protein (Fig. 3). We propose that the methylation of H2A.Z may possess the ability to associate properly with chromatin. H2A.Z mutants that cannot be methylated may easily dissociate from chromatin. These data suggest that H2A.ZK101 dimethylation may hinder its interaction with ANP32E, reduce the ANP32E-facilitated removal of H2A.Z, and allow H2A.Z to remain on the chromatin to execute their function in cyclin A1 activation (Fig. 6).

Cyclin A1 promotes G_1–S cell-cycle progression in somatic cells and overexpressed cyclin A1 enhances S-phase entry to provide an oncogenic effect in leukemia cells (48, 49). A previous study attributed cyclin A1–mediated cancer progression to dimethylation of H3K36 in the coding region of cyclin A1 gene, which increased cyclin A1 transcription (50). Here we identified H2A.ZK101me2 as another important epigenetic factor that positively regulates cyclin A1 expression. The loss of H2A.ZK101me2 lowered H2A.Z protein association with chromatin (Fig. 2). In addition, the net amounts of H2A.ZK101me2 and H2A.Z, but not those of H2A, H2B, H3, and H4, were decreased at the cyclin A1 promoter in SMYD3 knockdown or in H2A.ZK101-mutant cells (Fig. 5 and Supplementary Fig. S6). Consistently, overexpression of H2A.Z^{WT} proteins promoted cyclin A1 gene expression (Fig. 5C). Therefore, we suggest that the enrichment of H2A.ZK101me2 at the cyclin A1 promoter is an active mark for gene expression.

Disclosure of Potential Conflicts of Interest

No potential conflicts of interest were disclosed.

Authors' Contributions

Conception and design: C.-H. Tsai, Y.-J. Chen, M.-C. Lin, K.-J. Wu, S.-C. Teng
Development of methodology: C.-H. Tsai, Y.-J. Chen, S.-C. Teng
Acquisition of data (provided animals, acquired and managed patients, provided facilities, etc.): C.-H. Tsai, Y.-J. Chen, S.-R. Tzeng, W.-H. Kuo, M.-C. Lin
Analysis and interpretation of data (e.g., statistical analysis, biostatistics, computational analysis): C.-H. Tsai, Y.-J. Chen, C.-J. Yu, S.-R. Tzeng, M.-C. Lin, N.-L. Chan, K.-J. Wu, S.-C. Teng
Writing, review, and/or revision of the manuscript: C.-H. Tsai, Y.-J. Chen, M.-C. Lin, K.-J. Wu, S.-C. Teng
Administrative, technical, or material support (i.e., reporting or organizing data, constructing databases): Y.-J. Chen
Study supervision: Y.-J. Chen, S.-C. Teng
Other (protein purification): I-C. Wu

Acknowledgments

We thank Drs. Luc Gaudreau, Cheng-Fu Kao, Ming-Shyue Lee, Tsai-Kun Li, Hsueh-Fen Juan, and Ali Hamiche for providing materials. We also thank Dr. Li-Jung Juan for her critical comments on the manuscript.

Grant Support

This work was supported by a grant from National Health Research Institute of Taiwan (NHRI-EX101-9727BI to S.-C. Teng).

The costs of publication of this article were defrayed in part by the payment of page charges. This article must therefore be hereby marked *advertisement* in accordance with 18 U.S.C. Section 1734 solely to indicate this fact.

Received February 21, 2016; revised July 9, 2016; accepted August 6, 2016; published OnlineFirst August 28, 2016.

References

1. Morgan MA, Shilatifard A. Chromatin signatures of cancer. Genes Dev 2015;29:238–49.
2. Jones PA. Functions of DNA methylation: islands, start sites, gene bodies and beyond. Nat Rev Genet 2012;13:484–92.
3. Vardabasso C, Hasson D, Ratnakumar K, Chung CY, Duarte LF, Bernstein E. Histone variants: emerging players in cancer biology. Cell Mol Life Sci 2014;71:379–404.
4. Kouzarides T. Chromatin modifications and their function. Cell 2007; 128:693–705.
5. Valk-Lingbeek ME, Bruggeman SWM, van Lohuizen M. Stem cells and cancer: the polycomb connection. Cell 2004;118:409–18.
6. Kondo Y, Shen L, Suzuki S, Kurokawa T, Masuko K, Tanaka Y, et al. Alterations of DNA methylation and histone modifications contribute to gene silencing in hepatocellular carcinomas. Hepatology Res 2007;37: 974–83.
7. Kondo Y, Shen L, Ahmed S, Boumber Y, Sekido Y, Haddad BR, et al. Downregulation of histone H3 lysine 9 methyltransferase G9a induces centrosome disruption and chromosome instability in cancer cells. PLoS One 2008;3:e2037.
8. Krivtsov AV, Armstrong SA. MLL translocations, histone modifications and leukaemia stem-cell development. Nat Rev Cancer 2007;7:823–33.
9. Liu L, Kimball S, Liu H, Holowatyj A, Yang ZQ. Genetic alterations of histone lysine methyltransferases and their significance in breast cancer. Oncotarget 2015;6:2466–82.
10. Vieira FQ, Costa-Pinheiro P, Almeida-Rios D, Graca I, Monteiro-Reis S, Simoes-Sousa S, et al. SMYD3 contributes to a more aggressive phenotype of prostate cancer and targets Cyclin D2 through H4K20me3. Oncotarget 2015;6:13644–57.
11. Hamamoto R, Furukawa Y, Morita M, Iimura Y, Silva FP, Li M, et al. SMYD3 encodes a histone methyltransferase involved in the proliferation of cancer cells. Nat Cell Biol 2004;6:731–40.
12. Frank B, Hemminki K, Wappenschmidt B, Klaes R, Meindl A, Schmutzler RK, et al. Variable number of tandem repeats polymorphism in the SMYD3 promoter region and the risk of familial breast cancer. Int J Cancer 2006;118:2917–8.
13. Sarris ME, Moulos P, Haroniti A, Giakountis A, Talianidis I. Smyd3 is a transcriptional potentiator of multiple cancer-promoting genes and required for liver and colon cancer development. Cancer Cell 2016;29: 354–66.
14. Cock-Rada AM, Medjkane S, Janski N, Yousfi N, Perichon M, Chaussepied M, et al. SMYD3 promotes cancer invasion by epigenetic upregulation of the metalloproteinase MMP-9. Cancer Res 2012;72:810–20.
15. Van Aller GS, Reynoird N, Barbash O, Huddleston M, Liu S, Zmoos AF, et al. Smyd3 regulates cancer cell phenotypes and catalyzes histone H4 lysine 5 methylation. Epigenetics 2012;7:340–3.
16. Foreman KW, Brown M, Park F, Emtage S, Harriss J, Das C, et al. Structural and functional profiling of the human histone methyltransferase SMYD3. PLoS One 2011;6:e22290.

17. Kim H, Heo K, Kim JH, Kim K, Choi J, An W. Requirement of histone methyltransferase SMYD3 for estrogen receptor-mediated transcription. J Biol Chem 2009;284:19867–77.
18. Liu C, Fang X, Ge Z, Jalink M, Kyo S, Bjorkholm M, et al. The telomerase reverse transcriptase (hTERT) gene is a direct target of the histone methyltransferase SMYD3. Cancer Res 2007;67:2626–31.
19. Mazur PK, Reynoird N, Khatri P, Jansen PW, Wilkinson AW, Liu S, et al. SMYD3 links lysine methylation of MAP3K2 to Ras-driven cancer. Nature 2014;510:283–7.
20. Hua S, Kallen CB, Dhar R, Baquero MT, Mason CE, Russell BA, et al. Genomic analysis of estrogen cascade reveals histone variant H2A.Z associated with breast cancer progression. Mol Syst Biol 2008;4:188.
21. Valdes-Mora F, Song JZ, Statham AL, Strbenac D, Robinson MD, Nair SS, et al. Acetylation of H2A.Z is a key epigenetic modification associated with gene deregulation and epigenetic remodeling in cancer. Genome Res 2012;22:307–21.
22. Yang HD, Kim PJ, Eun JW, Shen Q, Kim HS, Shin WC, et al. Oncogenic potential of histone-variant H2A.Z.1 and its regulatory role in cell cycle and epithelial-mesenchymal transition in liver cancer. Oncotarget 2016;7:11412–23.
23. Kim K, Punj V, Choi J, Heo K, Kim JM, Laird PW, et al. Gene dysregulation by histone variant H2A.Z in bladder cancer. Epigenetics Chromatin 2013;6:34.
24. Horikoshi N, Sato K, Shimada K, Arimura Y, Osakabe A, Tachiwana H, et al. Structural polymorphism in the L1 loop regions of human H2A.Z.1 and H2A.Z.2. Acta Crystallogr D Biol Crystallogr 2013;69:2431–9.
25. Dryhurst D, Ishibashi T, Rose KL, Eirin-Lopez JM, McDonald D, Silva-Moreno B, et al. Characterization of the histone H2A.Z-1 and H2A.Z-2 isoforms in vertebrates. BMC Biol 2009;7:86.
26. Vardabasso C, Gaspar-Maia A, Hasson D, Punzeler S, Valle-Garcia D, Straub T, et al. Histone variant H2A.Z.2 mediates proliferation and drug sensitivity of malignant melanoma. Mol Cell 2015;59:75–88.
27. Ruhl DD, Jin J, Cai Y, Swanson S, Florens L, Washburn MP, et al. Purification of a human SRCAP complex that remodels chromatin by incorporating the histone variant H2A.Z into nucleosomes. Biochemistry 2006;45:5671–7.
28. Liang X, Shan S, Pan L, Zhao J, Ranjan A, Wang F, et al. Structural basis of H2A.Z recognition by SRCAP chromatin-remodeling subunit YL1. Nat Struct Mol Biol 2016;23:317–23.
29. Obri A, Ouararhni K, Papin C, Diebold ML, Padmanabhan K, Marek M, et al. ANP32E is a histone chaperone that removes H2A.Z from chromatin. Nature 2014;505:648–53.
30. Latrick CM, Marek M, Ouararhni K, Papin C, Stoll I, Ignatyeva M, et al. Molecular basis and specificity of H2A.Z-H2B recognition and deposition by the histone chaperone YL1. Nat Struct Mol Biol 2016;23:309–16.
31. Dryhurst D, McMullen B, Fazli L, Rennie PS, Ausio J. Histone H2A.Z prepares the prostate specific antigen (PSA) gene for androgen receptor-mediated transcription and is upregulated in a model of prostate cancer progression. Cancer Lett 2012;315:38–47.
32. Draker R, Ng MK, Sarcinella E, Ignatchenko V, Kislinger T, Cheung P. A combination of H2A.Z and H4 acetylation recruits Brd2 to chromatin during transcriptional activation. PLoS Genet 2012;8:e1003047.
33. Schnitzler GR. Isolation of histones and nucleosome cores from mammalian cells. Curr Protoc Mol Biol 2001;Chapter 21:Unit 21 5.
34. Brown MA, Sims RJIII, Gottlieb PD, Tucker PW. Identification and characterization of Smyd2: a split SET/MYND domain-containing histone H3 lysine 36-specific methyltransferase that interacts with the Sin3 histone deacetylase complex. Mol Cancer 2006;5:26.
35. Jensen K, Santisteban MS, Urekar C, Smith MM. Histone H2A.Z acid patch residues required for deposition and function. Mol Genet Genomics 2011;285:287–96.
36. Wang AY, Aristizabal MJ, Ryan C, Krogan NJ, Kobor MS. Key functional regions in the histone variant H2A.Z C-Terminal docking domain. Mol Cell Biol 2011;31:3871–84.
37. Subramanian V, Mazumder A, Surface LE, Butty VL, Fields PA, Alwan A, et al. H2A.Z acidic patch couples chromatin dynamics to regulation of gene expression programs during ESC differentiation. Plos Genet 2013;9:e1003725.
38. Park YJ, Chodaparambil JV, Bao Y, McBryant SJ, Luger K. Nucleosome assembly protein 1 exchanges histone H2A-H2B dimers and assists nucleosome sliding. J Biol Chem 2005;280:1817–25.
39. Hoch DA, Stratton JJ, Gloss LM. Protein-protein Forster resonance energy transfer analysis of nucleosome core particles containing H2A and H2A.Z. J Mol Biol 2007;371:971–88.
40. Wong MM, Cox LK, Chrivia JC. The chromatin remodeling protein, SRCAP, is critical for deposition of the histone variant H2A.Z at promoters. J Biol Chem 2007;282:26132–9.
41. Auger A, Galarneau L, Altaf M, Nourani A, Doyon Y, Utley RT, et al. Eaf1 is the platform for NuA4 molecular assembly that evolutionarily links chromatin acetylation to ATP-dependent exchange of histone H2A variants. Mol Cell Biol 2008;28:2257–70.
42. Mao Z, Pan L, Wang W, Sun J, Shan S, Dong Q, et al. Anp32e, a higher eukaryotic histone chaperone directs preferential recognition for H2A.Z. Cell Res 2014;24:389–99.
43. Suto RK, Clarkson MJ, Tremethick DJ, Luger K. Crystal structure of a nucleosome core particle containing the variant histone H2A.Z. Nat Struct Biol 2000;7:1121–4.
44. Ren TN, Wang JS, He YM, Xu CL, Wang SZ, Xi T. Effects of SMYD3 overexpression on cell cycle acceleration and cell proliferation in MDA-MB-231 human breast cancer cells. Med Oncol 2011;28 Suppl 1:S91–8.
45. Zlatanova J, Thakar A. H2A.Z: view from the top. Structure 2008;16:166–79.
46. Svotelis A, Gevry N, Grondin G, Gaudreau L. H2A.Z overexpression promotes cellular proliferation of breast cancer cells. Cell Cycle 2010;9:364–70.
47. Nagata DE, Ting HA, Cavassani KA, Schaller MA, Mukherjee S, Ptaschinski C, et al. Epigenetic control of Foxp3 by SMYD3 H3K4 histone methyltransferase controls iTreg development and regulates pathogenic T-cell responses during pulmonary viral infection. Mucosal Immunol 2015;8:1131–43.
48. Holm C, Ora I, Brunhoff C, Anagnostaki L, Landberg G, Persson JL. Cyclin A1 expression and associations with disease characteristics in childhood acute lymphoblastic leukemia. Leuk Res 2006;30:254–61.
49. Ji P, Agrawal S, Diederichs S, Baumer N, Becker A, Cauvet T, et al. Cyclin A1, the alternative A-type cyclin, contributes to G1/S cell cycle progression in somatic cells. Oncogene 2005;24:2739–44.
50. Hsia DA, Tepper CG, Pochampalli MR, Hsia EYC, Izumiya C, Huerta SB, et al. KDM8, a H3K36me2 histone demethylase that acts in the cyclin A1 coding region to regulate cancer cell proliferation. Proc Natl Acad Sci 2010;107:9671–76.